Dual-band planar electric metamaterial in the terahertz regime

Yu Yuan[1], Christopher Bingham[2], Talmage Tyler[1], Sabarni Palit[1], Thomas H. Hand[1], Willie J. Padilla[2], David R. Smith[1], Nan Marie Jokerst[1], and Steven A. Cummer[1]

[1]*Center for Metamaterials and Integrated Plasmonics and Department of Electrical and Computer Engineering, Duke University, Durham, North Carolina, 27708*

[2]*Department of Physics, Boston College, Chestnut Hill, Massachusetts, 02467*

yuyuan.06@gmail.com

Abstract: We present the design, fabrication, and measurement of a dual-band planar metamaterial with two distinct electric resonances at 1.0 and 1.2 THz, as a step towards the development of frequency agile or broadband THz materials and devices. A method of defining the effective thickness of the metamaterial layer is introduced to simplify the material design and characterization. Good agreement between the simulated and measured transmission is obtained for the fabricated sample by treating the sample as multi-layer system, i. e. the effective metamaterial layer plus the rest of the substrate, as well as properly modeling the loss of the substrate. The methods introduced in this paper can be extended to planar metamaterial structures operating in infrared and optical frequency ranges.

OCIS codes: (160.1245) Artificially engineered materials; (160.3918) Metamaterials

References and links

1. V. G. Veselago, "The electrodynamics of substance with simultaneously negative value of ε and μ," Sov. Phys. Usp. **10**, 509-514 (1968).
2. J. B. Pendry, A. J. Holden, W. J. Stewart, and I. Youngs, "Extremely Low Frequency Plasmons in Metallic Mesostructures," Phys. Rev. Lett. **76**, 4773-4776 (1996).
3. J. B. Pendry, A. J. Holden, D. J. Robbins, and W. J. Stewart, "Magnetism from conductors and enhanced nonlinear phenomena," IEEE Trans. Microwave Theory Tech. **47**, 2075-2084 (1999).
4. D. R. Smith, W. J. Padilla, D. C. Vier, S. C. Nemat-Nasser, and S. Schultz, "Composite medium with simultaneously negative permeability and permittivity," Phys. Rev. Lett. **84**, 4184-4187 (2000).
5. R. A. Shelby, D. R. Smith, and S. Shultz, "Experimental verification of a negative index of refraction," Science **292**, 77-79 (2001).
6. S. A. Cummer and B. I. Popa, "Wave fields measured inside a negative refractive index metamaterial," Appl. Phys. Lett. **85**, 4564-4566 (2004).
7. Y. Yuan, L. Ran, H. Chen, J. Huangfu, T. M. Grzegorczyk, and J. A. Kong, "Backward coupling waveguide coupler using left-handed material," Appl. Phys. Lett. **88**, 211903 (2006).
8. H. Chen, B. I. Wu, L. Ran, T. M. Grzegorczyk, and J. A. Kong, "Controllable left-handed metamaterial and its application to a steerable antenna," Appl. Phys. Lett. **89**, 053509 (2006).
9. T. J. Yen, W. J. Padilla, N. Fang, D. C. Vier, D. R. Smith, J. B. Pendry, D. N. Basov, and X. Zhang, "Terahertz magnetic response from artificial materials," Science **303**, 1494-1496 (2004).
10. H. O. Moser, B. D. F. Casse, O. Wilhelmi, and B. T. Saw, "Terahertz response of a microfabricated rod-split-ring-resonator electromagnetic metamaterial," Phys. Rev. Lett. **94**, 063901 (2005).
11. W. J. Padilla, A. J. Taylor, C. Highstrete, M. Lee, and R. D. Averitt, "Dynamical electric and magnetic metamaterial response at terahertz frequencies," Phys. Rev. Lett. **96**, 107401 (2006).

#95873 - $15.00 USD Received 8 May 2008; revised 10 Jun 2008; accepted 11 Jun 2008; published 17 Jun 2008

12. H.-T. Chen, W. J. Padilla, J. M. O. Zide, A. C. Gossard, A. J. Taylor, and R. D. Averitt, "Active terahertz metamaterial devices," Nature **444**, 597-600 (2006)
13. R. Marqués, F. Medina, and R. Rafii-El-Idrissi, "Role of bianisotropy in negative permeability and left-handed metamaterials," Phys. Rev. B **65**, 144440 (2002).
14. J. García-García, F. Martín, J. D. Baena, R. Maqués, and L. Jelinek, "On the resonances and polarizabilities of split ring resonators," J. Appl. Phys. **98**, 033103 (2005).
15. K. A. McIntosh, E. R. Brown, K. B. Nichols, O. B. McMahon, W. F. DiNatale, and T. M. Lyszczarz, "Terahertz measurements of resonant planar antennas coupled to low-temperature-grown GaAs photomixers," Appl. Phys. Lett. **69**, 3632-3634 (1996).
16. T. Driscoll, D. N. Basov, W. J. Padilla, J. J. Mock, and D. R. Smith, "Electromagnetic characterization of planar metamaterials by oblique angle spectroscopic measurements," Phys. Rev. B **75**, 115114 (2007).
17. T. Driscoll, G. O. Andreev, D. N. Basov, S. Palit, Tong Ren, Jack Mock, Sang-Yeon Cho, Nan Marie Jokerst, and D. R. Smith, "Quantitative investigation of terahertz artificial magnetic resonance using oblique angle spectroscopy," Appl. Phys. Lett. **90**, 092508 (2007).
18. B. Popa and S. A. Cummer, "Determining the effective electromagnetic properties of negative-refractive-index metamaterials from internal fields," Phys. Rev. B **72**, 165102 (2005).
19. M. Gorkunov, M. Lapine, E. Shamonina, and K. H. Ringhofer, "Effective magnetic properties of a composite material with circular conductive elements," Eur. Phys. J. B **28**, 263-269 (2002).
20. D. R. Smith, S. Schultz, P. Marko, and C. M. Soukoulis, "Determination of effective permittivity and permeability of metamaterials from reflection and transmission coefficients," Phys. Rev. B **65**, 195104 (2002).
21. X. Chen, T. M. Grzegorczyk, B.-I. Wu, J. Pacheco, and J. A. Kong, "Robust method to retrieve the constitutive effective parameters of metamaterials," Phys. Rev. E **70**, 016608 (2004).
22. D. R. Smith, D. C. Vier, Th. Koschny, and C. M. Soukoulis, "Electromagnetic parameter retrieval from inhomogeneous metamaterials," Phys. Rev. E **71**, 036617 (2005).

1. Introduction

Artificial electromagnetic structures, called metamaterials, can be engineered to exhibit exotic electric and magnetic properties not realizable in nature [1, 2, 3, 4, 5]. Most early developments in metamaterials operated in the microwave regime [6, 7, 8] due to the simplicity in fabrication and measurement. Metamaterials that operate at terahertz (THz) frequencies are attractive [9, 10, 11], since most materials found in nature are transparent to electromagnetic radiation at these frequencies, and metamaterials are candidates to fill this "terahertz gap". For example, metamaterials were employed to exhibit real-time control and manipulation of terahertz radiation [12].

Terahertz metamaterials thus far reported have exhibited single-band electric or magnetic responses. As a step towards frequency agile or broadband THz materials and devices, we present here the design, fabrication, and measurement of a dual-band planar electric metamaterial that has two distinct resonances at 1.0 and 1.2 THz. A method to define the effective thickness of the metamaterial layer is also introduced, which substantially simplifies the material design and characterization. Furthermore, we demonstrate that by treating the fabricated sample as multilayer system, i.e. the effective metamaterial layer plus the rest of the substrate layer, as well as properly modeling the loss of the substrate, extremely good agreement between the simulated and measured transmission through the sample is obtained. The methods introduced in this paper are general and can be extended to planar metamaterial structures in the infrared and optical frequency ranges.

2. Dual-band electric resonator

Metallic split ring resonators (SRRs) at a scale of several tens of microns (μm) can be used to excite a magnetic response at terahertz frequencies [9, 10, 11]. These SRRs are inherently bianisotropic, however, the magnetoelectric coupling can be eliminated by making a symmetrical structure consisting of two opposed SRRs [13]. Planar metamaterials can be formed by patterning arrays of symmetrical SRRs on a dielectric substrate. The metamaterial surface has an in-plane electric resonant response and an out-of-plane magnetic response for normal trans-

#95873 - $15.00 USD Received 8 May 2008; revised 10 Jun 2008; accepted 11 Jun 2008; published 17 Jun 2008

verse electromagnetic (TEM) incidence. In this case, if the electric field is orthogonal to the SRR gaps, the response of the structure is purely electric, and since the incident magnetic field is parallel to the SRR plane, it does not couple to the SRRs. Thus, symmetrical SRRs contain electric resonances that enable control over the permittivity of a metamaterial.

Using two different sized symmetric SRRs, two distinct resonant frequencies can be excited. Unlike dual-band (not electrical) resonances achieved through higher-order modes with some topologies of the SRR [14], both of the resonances in the proposed structure are fundamental resonant modes (the quasistatic resonance). A unit cell of the dual-band electric metamaterial was designed using *Ansoft* HFSS, a commercial finite element-based electromagnetic field solver.

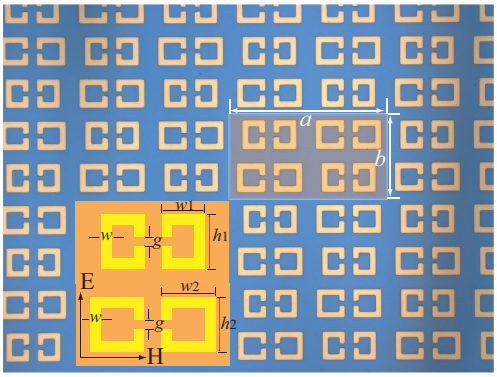

Fig. 1. Photomicrograph of the fabricated dual symmetrical SRR sample. A unit cell of the metamaterial is shown in the highlighted, white-edged box, and inset is the simulated SRRs, polarization of the incident wave included. Lattice constants of the unit cell $a = 112\ \mu m$ and $b = 60\ \mu m$, and geometric parameters of the SRRs are: $w_1 = 16\ \mu m$, $h_1 = w_2 = h_2 = 20\ \mu m$, $w = 4\ \mu m$, and $g = 3\ \mu m$.

The lattice constants of the unit cell were $a = 112\ \mu m$ and $b = 60\ \mu m$. The SRRs were designed as follows: the dimension of the large SRRs was $20\ \mu m \times 20\ \mu m$ (outer) and $12\ \mu m \times 12\ \mu m$ (inner), and that of the small SRRs was $20\ \mu m \times 16\ \mu m$ (outer) and $12\ \mu m \times 8\ \mu m$ (inner), respectively. The gaps in the SRRs were $3\ \mu m$. The designed SRR structure and the polarization of the incident electromagnetic (EM) wave are shown in the inset in Fig. 1. All the metal traces consisted of titanium/platinum/gold layers (thicknesses: 30 nm/40 nm/200 nm) in the simulation. The dielectric constant of GaAs was assumed to be $\varepsilon_r = 12.8$ (real part) [15], and the loss tangent was assumed to be 0.006.

3. Effective metamaterial layer and parameter retrieval

Simulation of the metamaterial was complicated by the thickness of the GaAs substrate. Therefore, rather than simulate the physical medium exactly, the metamaterial was instead treated as a multilayer system [16, 17]: a metamaterial layer (which includes the metal SRRs and the adjacent substrate and air layers), plus the GaAs substrate. The effective thickness of the metamaterial layer was defined by how far the SRR-induced fields extend above and below the SRR plane. It was reported in [18, 19] that this thickness is roughly equal to the in-plane SRR periodicity, P. However, this method requires that the field distribution be known from the simulation model at various frequencies near resonance, and defining the periodicity P can be difficult, especially for complex structures.

For simplicity, we propose a method of approximately defining the effective thickness of the

#95873 - $15.00 USD Received 8 May 2008; revised 10 Jun 2008; accepted 11 Jun 2008; published 17 Jun 2008

planar THz metamaterial. The effective thickness of the substrate was defined based on the convergence of the resonant frequency for different thicknesses. To simplify the procedure, only the large symmetrical SRRs were simulated, with a substrate thickness of 5 μm, 10 μm, and 20 μm, respectively. The calculated transmission properties revealed that the resonant frequency converged when the substrate thickness was 10 μm (for large symmetrical SRRs, the resonant frequency shifted less than one percent when the substrate thickness was increased to 20 μm). This means that the 10 μm-thick substrate provides sufficient capacitance for the gaps of the SRRs, and adding more substrate thickness does not modify the local fields of the SRRs. The fields radiated by the SRRs were negligible, considering that the dimensions of the SRRs were less than 1/10 of the free space wavelength, thus most of the SRR-induced fields extend within 10 μm into the GaAs substrate. For the air layer, a thickness equal to that of the substrate (10 μm) was used because even this short distance is long enough that quasistatic fields in the air layer have decayed substantially. This makes the effective thickness of the metamterial layer 20 μm, which is equal to the dimensions of the large SRRs as is typical for many metamaterial designs. The effective thickness of the metamaterial layer roughly defined by this method in the planar terahertz metamaterials simplifies the design procedure. The electromagnetic characteristics of the metamaterial layer can also be easily obtained, and will be shown later.

Figure 2(a) shows the simulated transmission properties of the metamaterial layer shown in Fig. 1. This transmission was calculated based on a three-layer configuration (air/metamaterial layer/air) to obtain the reflection and transmission of the metamaterial layer for the extraction of the EM parameters.

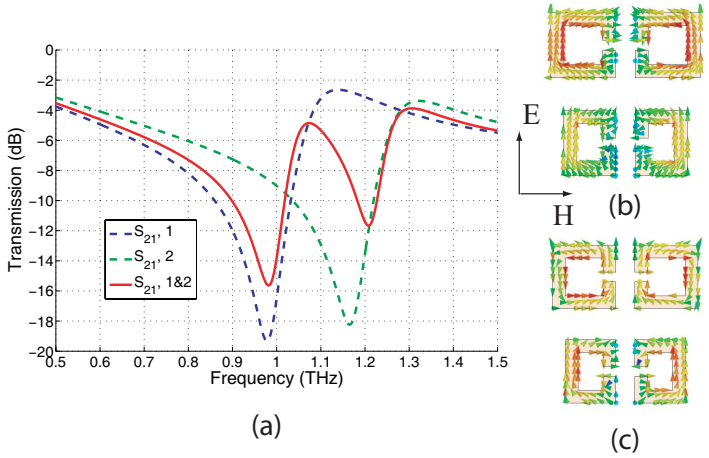

Fig. 2. (a) Simulated transmission (in dB) of the dual-band electric metamaterial (solid line), and of the individual symmetrical SRRs (dashed lines). (b) Surface current circulation on the symmetrical SRRs near $f_{o,1}$, and (c) surface current circulation on the symmetrical SRRs near $f_{o,2}$.

In the simulation, periodic boundaries (master/slave in the Ansoft HFSS) were assigned on the four surfaces perpendicular to the SRR plane, and two waveguide ports were constructed and used along the direction of wave propagation. The transmission obtained is not identical to the transmission of the full sample, and this will be discussed later. As shown in Fig. 2, two resonant frequencies, $f_{o,1} = 0.99$ THz and $f_{o,2} = 1.21$ THz, are excited for the large and small symmetrical SRRs, respectively. The calculated transmission through layers composed solely of individual large and small symmetrical SRRs is also shown in Fig. 2 (dashed lines) and these resonances occur at $f_{o,1} = 0.98$ THz and $f_{o,2} = 1.17$ THz.

#95873 - $15.00 USD Received 8 May 2008; revised 10 Jun 2008; accepted 11 Jun 2008; published 17 Jun 2008

The theoretical resonances for the dual resonance sample are slightly blue shifted (the shift of the first resonance is approximately 4 GHz). The two resonances are about 3.7 dB and 6.6 dB weaker than those simulated for layers completely filled with single resonance particles. This is expected because the volume concentration of each type of resonator in the dual band sample is half of that for a layer completely filled with a single type of resonator. The second resonance is weakened further in the dual band structure due to interactions between the two resonators. Due to the existing mutual inductance between the two different symmetrical SRRs, the resonant particles (large symmetrical SRRs) induce the same-direction surface current circulation on the non-resonant particles near the first resonance $f_{o,1}$, as seen in Fig. 2(b) (left). Near the second resonance $f_{o,2}$, the resonant particles (small symmetrical SRRs) induce the opposite-direction surface current circulation on the non-resonant SRR, as seen in Fig. 2(b) (right). Thus, near the second resonance, the electric resonance response of the small symmetrical SRRs is also weakened by the cancelation of the particle polarizability of the non-resonant large symmetrical SRRs. Therefore, even though the filling fraction decreases by a same factor for the two different symmetrical SRRs, the second resonance response is much more weakened than the first one.

For normally incident waves on the SRR plane, the structure is asymmetric along the direction of wave propagation. With the incoming wave facing either the SRR structure or the GaAs substrate, the transmission of the incident wave through the metamaterial layer is identical. In contrast, the reflection properties of the sample are slightly different, based upon whether the incident wave is incident on the SRR structure or on the GaAs substrate. Here, a standard retrieval algorithm [20, 21] was used to obtain the effective permittivity of the material (shown in Fig. 3), which is the permittivity a stack of many individual layers of our material would have,

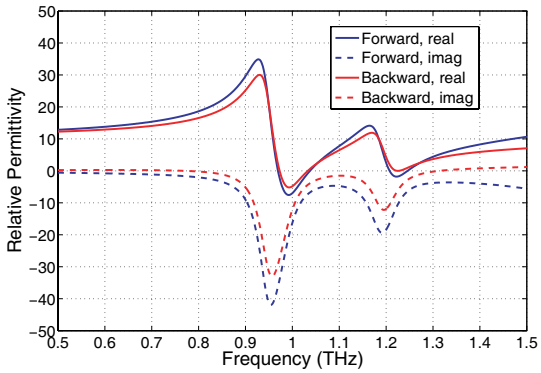

Fig. 3. Retrieved permittivity for the dual-band electric metamaterial, based on incidence from the symmetrical SRRs side (forward, blue lines), and from the substrate side (backward, red lines).

based on normal incidence from the SRR side (forward incidence, blue lines) as well as normal incidence from the substrate side (backward incidence, red lines). For the forward incidence, the real part of the retrieved permittivity yields values of –7.5 and –1.8 at the first and second resonances, respectively. The corresponding permittivity values for the backward wave incidence are –5.2 and –0.02. This difference is well-understood as a consequence of inhomogeneity of the structure along the directions of wave propagation in [22].

#95873 - $15.00 USD Received 8 May 2008; revised 10 Jun 2008; accepted 11 Jun 2008; published 17 Jun 2008

4. Fabrication, measurement, and simulation agreement

To fabricate the designed metamaterial, a metallic SRR structure was deposited and patterned on a 500 μm-thick GaAs substrate. The metal layer structure consisted of electron beam vacuum evaporated Ti/Pt/Au (thicknesses 30 nm/40 nm/200 nm). The titanium was used for good adhesion to the substrate, and platinum was used between the Ti and the Au to prevent intermetallic diffusion. Negative photolithography was used to define the SRR structures using metal lift-off in acetone and an ultrasonic agitator. A photomicrograph of the fabricated metamaterial sample is shown in Fig. 1.

A Bruker Vertex 80V FTIR spectrometer was used to make the measurements. The metamaterial sample was illuminated by a mercury lamp with a 4 mm aperture (a polarizer oriented in the vertical direction was placed in the beam path), and a Si-bolometer detector cooled with liquid helium was placed on the opposite side of the sample to measure the transmitted EM waves. The measured transmission of the fabricated planar metamaterial is shown in Fig. 4, and it is compared with the simulated transmission spectrum.

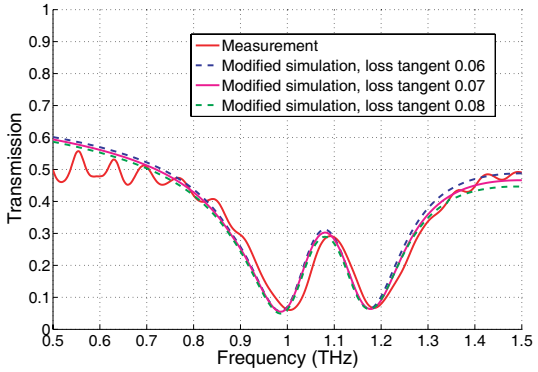

Fig. 4. Measured transmission for the fabricated sample (solid red line), and the simulated transmission spectrum for the modified models. In the modified simulation, the loss tangent of the extra GaAs substrate was swept: 0.06 (dashed blue line), 0.07 (solid pink line), and 0.08 (dashed green line).

It should be noted that the data obtained in the measurement was processed to remove portions of the signal caused by fresnel reflections. Because it is not feasible to simulate the full 500 μm thick fabricated sample, the transmission properties were modeled by adding an extra 40 μm-thickness of GaAs to the metal layer and 10 μm GaAs substrate. The loss tangent of this 40 μm layer was artificially increased to 0.07 to reproduce the same total loss as in the remaining 490 μm of GaAs substrate (loss tangent 0.006). Also in this simulation, periodic boundaries were assigned as previously, but a plane wave was excited, and two radiation ports, with one port attached on the GaAs substrate, were used along the direction of wave propagation. As shown in Fig. 4, the agreement between simulation and measurement is extremely good, with less than a shift of 0.02 THz between simulated and the measured resonant frequencies. The agreement in magnitude between the simulation and the measurement, whether near or away from the resonant frequencies, validates our assumption that the substrate loss tangent is 0.006 for the GaAs used in our fabrication. Other simulated transmission spectra on the figure show that the agreement is not very sensitive to the artificially increased loss tangent.

#95873 - $15.00 USD Received 8 May 2008; revised 10 Jun 2008; accepted 11 Jun 2008; published 17 Jun 2008

5. Conclusion

In conclusion, we report theoretical and experimental results for a 1.0 and 1.2 THz dual-band planar electric metamaterial. Material design and parameter analysis was explored, and the designed metamaterial sample was fabricated and characterized. The measured transmission was in good agreement with predictions from simulation. The design, fabrication, and measurement of a dual-band electric THz metamaterial presented here is a step towards frequency agile and broadband THz materials and devices.

#95873 - $15.00 USD Received 8 May 2008; revised 10 Jun 2008; accepted 11 Jun 2008; published 17 Jun 2008